Title

A human ex vivo skin model breaking boundaries.

Journal

Scientific Reports, 14(1)

Authors

Wurbs, Astrid
Karner, Christina
Vejzovic, Djenana
et al.

Publication Date

2024-10-14

DOI

10.1038/s41598-024-75291-7

Peer reviewed

scientific reports

Check for updates

OPEN

A human ex vivo skin model breaking boundaries

Astrid Wurbs[1], Christina Karner[1], Djenana Vejzovic[1], Georg Singer[2], Markus Pichler[3], Bernadette Liegl-Atzwanger[4] & Beate Rinner[1]✉

Ex vivo human skin models are valuable tools in skin research due to their physiological relevance. Traditionally, standard cultivation is performed in a cell culture incubator with a defined temperature of 37 °C and a specific atmosphere enriched with CO_2 to ensure media stability. Maintaining the model under these specific conditions limits its flexibility in assessing exposures to which the skin is exposed to in daily life, for example changes in atmospheric compositions. In this study we demonstrated that the foreskin-derived skin model can be successfully cultured at room temperature outside a CO_2 incubator using a CO_2-independent, serum-free media. Over a cultivation period of three days, the integrity of the tissue and the preservation of immune cells is well maintained, indicating the model's stability and resilience under the given conditions. Exposing our Medical University of Graz – human Organotypic Skin Explant Culture (MUG-hOSEC) model to cytotoxic and inflammatory stimuli results in responses analyzable within the supernatant. Besides the common analysis of released proteins upon treatment, such as cytokines and enzymes, we have included extracellular vesicle to obtain a more comprehensive picture of cell communication.

Keywords Ex vivo skin model, Juvenile foreskin, Room temperature, Extracellular vesicles

In vitro skin models cultured at air-liquid interface have two prominent representatives, the reconstructed human epidermis (RHE) and the more complex skin equivalent (SE) having an additional dermal layer. The RHE model is well established and commercially available. It serves well as a suitable replacement for animal testing in regards to the assessment of skin corrosion or skin irritation properties of a substance[1,2]. Although these models are valuable tools, they pose limitations towards advanced testing, such as skin diseases or wound healing. The lack of additional components of the native skin, certain cell types (for example, immune cells, nerve cells, adipocytes or melanocytes) or skin appendages (for example, hair follicles, sebaceous and sweat glands), as well as interacting systems namely vascularization, nerve system or native structural features (dermal matrix), limits their competence of prediction[3].

At this point, the ex vivo human skin model, an explant skin culture, prepared from left over skin after surgical interventions, compensates some of the missing features and provides a closer in vivo setting with a broad spectrum of applications. Even in cases where in vitro skin models can serve for evaluation, the ex vivo model provides deeper insight into underling mechanisms[4,5]. Especially the immunocompetence of the ex vivo skin models, achieved by resident immune cells present within the explant skin, is a huge benefit leading to an increase in accuracy and preclinical relevance[6–8]. In a small-scale scenario, various developed cultivation techniques have shown to provide results for the two most promising applications of the model, wound healing and inflammatory diseases. To name a few, the effect of new cosmetic technologies such as microneedling[9], the evaluation of wound healing gels[10] or new approaches towards psoriasis treatments[11] have been conducted. The models can also be used to investigate infections of fungi[12], viruses[13] or intradermal vaccination[14]. As the largest barrier organ, the skin is constantly exposed to the external environment, lifestyle, diet, sun exposure and other environmental factors affect the skin. In its natural environment, the skin is rarely exposed to 37 °C on its surface, and the temperature fluctuations are sometimes enormous. Our model is not exposed to stable temperature 37 °C settings and better mimics the in vivo situation. Furthermore, independence towards cell culture conditions broadens the fields of applications by facilitating the implementation of alternative testing conditions. Independence from a cell culture incubator could, for instance, facilitate testing the impact of air pollution on skin, a contributing factor to skin disorders[15–17].

Characterization and verification of the ex vivo skin model by different working groups were performed using individual culturing medium and techniques. In some cases the medium contains fetal calve serum[18–20]

[1]Division of Biomedical Research, Core Facility Alternative Biomodels and Preclinical Imaging, Medical University of Graz, Roseggerweg 48, 8036 Graz, Austria. [2]Department of Paediatric and Adolescent Surgery, Medical University of Graz, Graz, Austria. [3]Prototyping and Construction, Medical University of Graz, Graz, Austria. [4]Diagnostic and Research Institute of Pathology, Medical University of Graz, Graz, Austria. ✉email: beate.rinner@medunigraz.at

in other cases a defined, serum-free medium, complemented with or without different components[21–24] is used. In summary, different cultivation media can be seen, but always the same cultivation conditions with regards to temperature (37 °C) and CO_2 incubator (5 %), concluding a general robustness towards medium requirements. CO_2 independent media used for the MUG-hOSEC (Medical University of Graz – human Organotypic Skin Explant Culture) model does not require specific media adjustments to compensate CO_2 buffering. We demonstrate that the ex vivo skin model, derived from foreskin samples, can be maintained in a CO_2 independent media cultivated at room temperature. As there are multiple applications for ex vivo skin models, we opted for a short cultivation period, enabling tests on the cytotoxic or inflammatory effects of external stimuli.

Besides the standardized measurement of changes in cytokine expression or the release of cytoplasmic enzymes in response to cytotoxic and inflammatory insults, this study aims to introduce extracellular vesicle (EVs) measurement as an additional parameter for monitoring cell status. Skin cells communicate via EVs during wound healing and inflammation[25–27]. Having the opportunity to cultivate explant skin with all its in vivo components and monitoring effects of treatments on multiple levels will further improve preclinical relevance, making the models interesting for even more applications.

Results

The challenge of heterogeneity and reproducibility of the MUG-hOSEC (Medical University of Graz – human Organotypic Skin Explant Culture) model

The ex vivo skin model presented in this study is derived from foreskin samples. Figure 1 provides an overview of the workflow from the surgery to the final MUG-hOSEC model, to the characterization and possible readouts. On average, four to five skin punches with a 8 mm diameter could be extracted from each sample. The received skin punches exhibit optical heterogeneity in terms of color, shape, thickness and signs of vascularization. These variations are observed not only between different donors but also within the same donor. The epidermal thickness and structure can vary significantly between two donors, as illustrated in haematoxylin and eosin (H&E) stains (Fig. 2).

To enhance comparative possibilities, skin punches were weighed before being transferred into the trans-well insert. The mean weight of 39 skin punches was 90.2 ± 18.2 mg. A summary of all data obtained from each skin punch is provided in the supplementary files, Table S1. Normalization to skin punch weight of the individual results obtained from one skin punch was only performed for total secreted particles (Nanoparticle Tracking Analysis (NTA)). The relation of weight to other released factors has to be further examined and was therefore not included in this study.

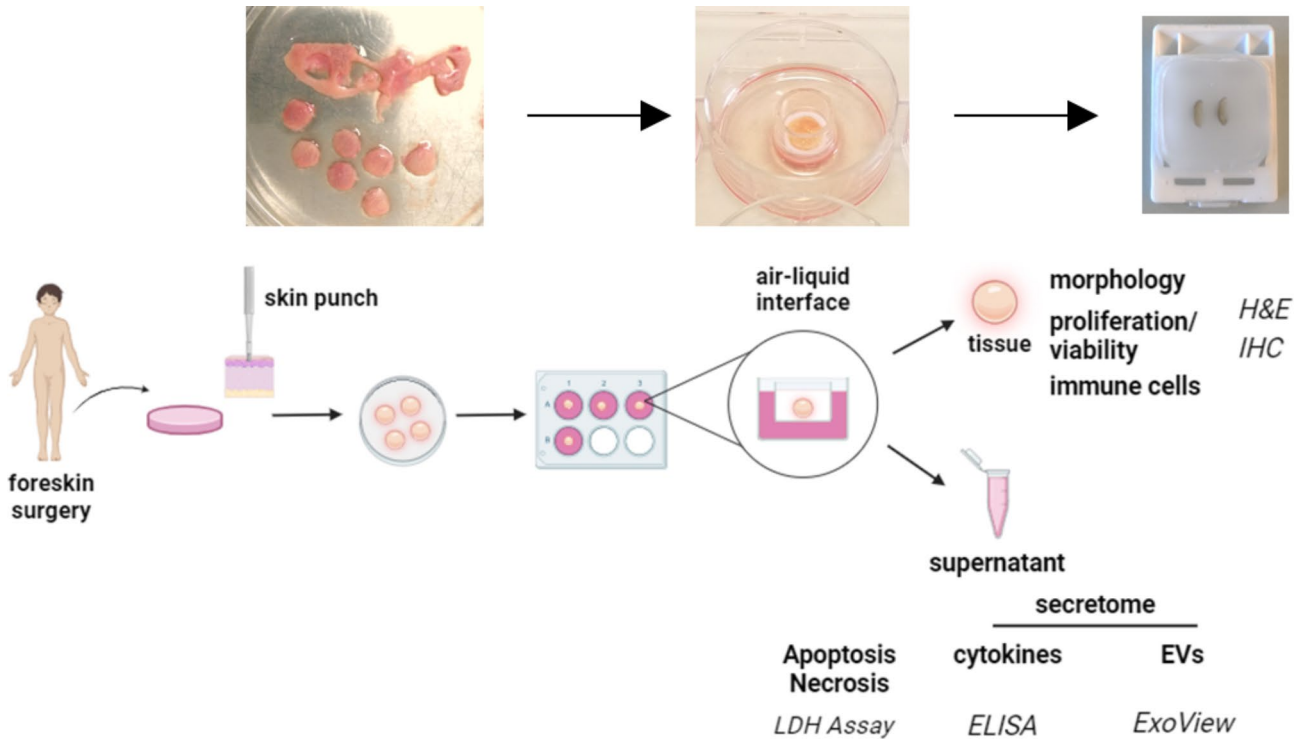

Fig. 1. Standardized workflow for preparing and utilizing the MUG-hOSEC model. Schematic overview from surgery to preparation with exemplary pictures. Readouts after treatment can be derived from the skin tissue itself or the analysis of the supernatant.

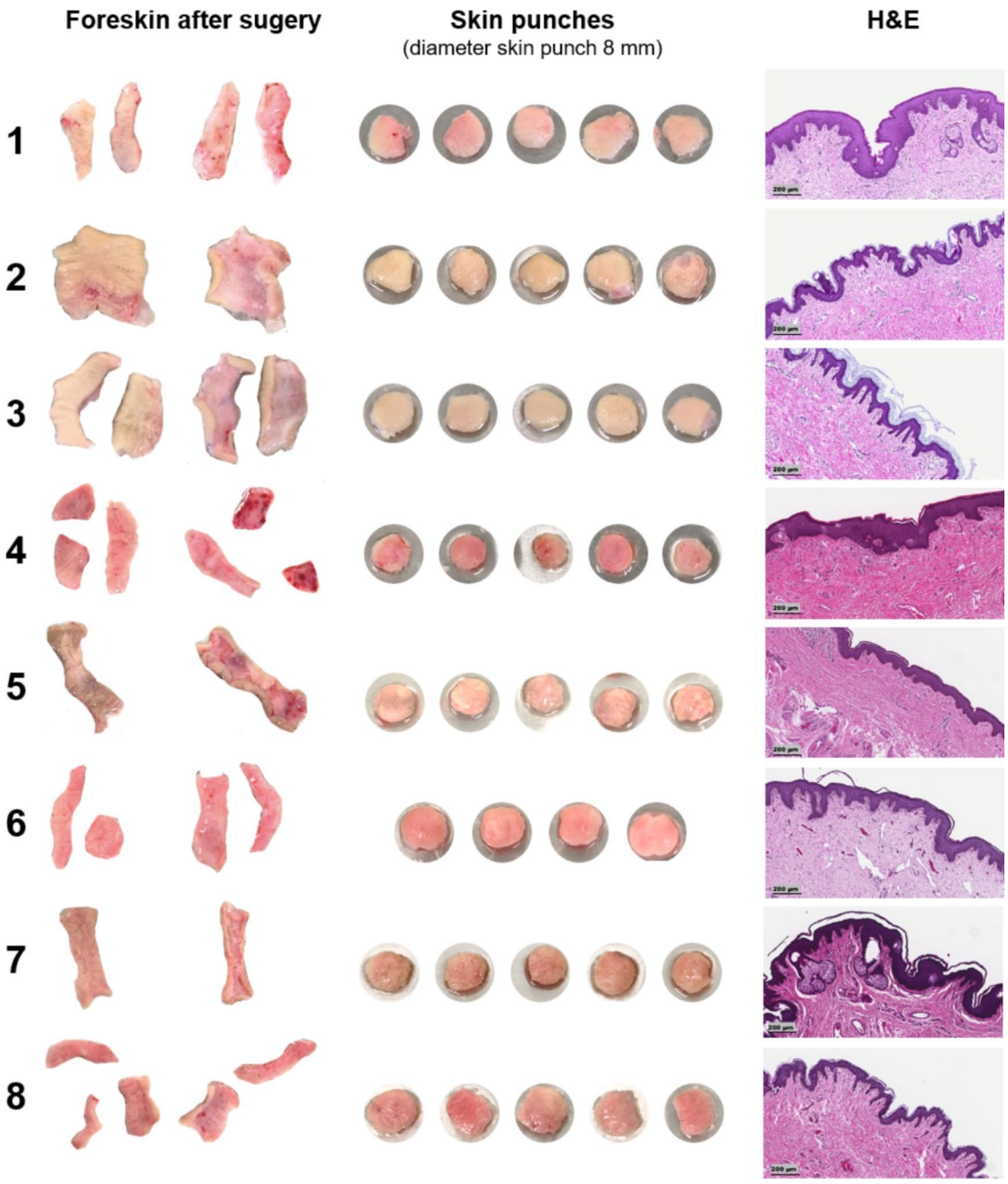

Fig. 2. Heterogeneity of the obtained foreskin samples. Images depict the epidermal and dermal side of washed and disinfected foreskin samples, with respective obtained skin punches using an 8 mm skin punch. Corresponding haematoxylin and eosin (H&E) staining on the day of receiving the foreskin. Magnification x10, Scale bar 200 µm.

Proof of integrity through morphological investigation

To confirm the preservation of skin integrity under the established cultivation conditions and within the cultivation time frame of three days, histological parameters describing the tissue structure (haematoxylin and eosin (H&E) staining) and tissue viability (KI-67 and Caspase-3 staining) were assessed (Fig. 3).

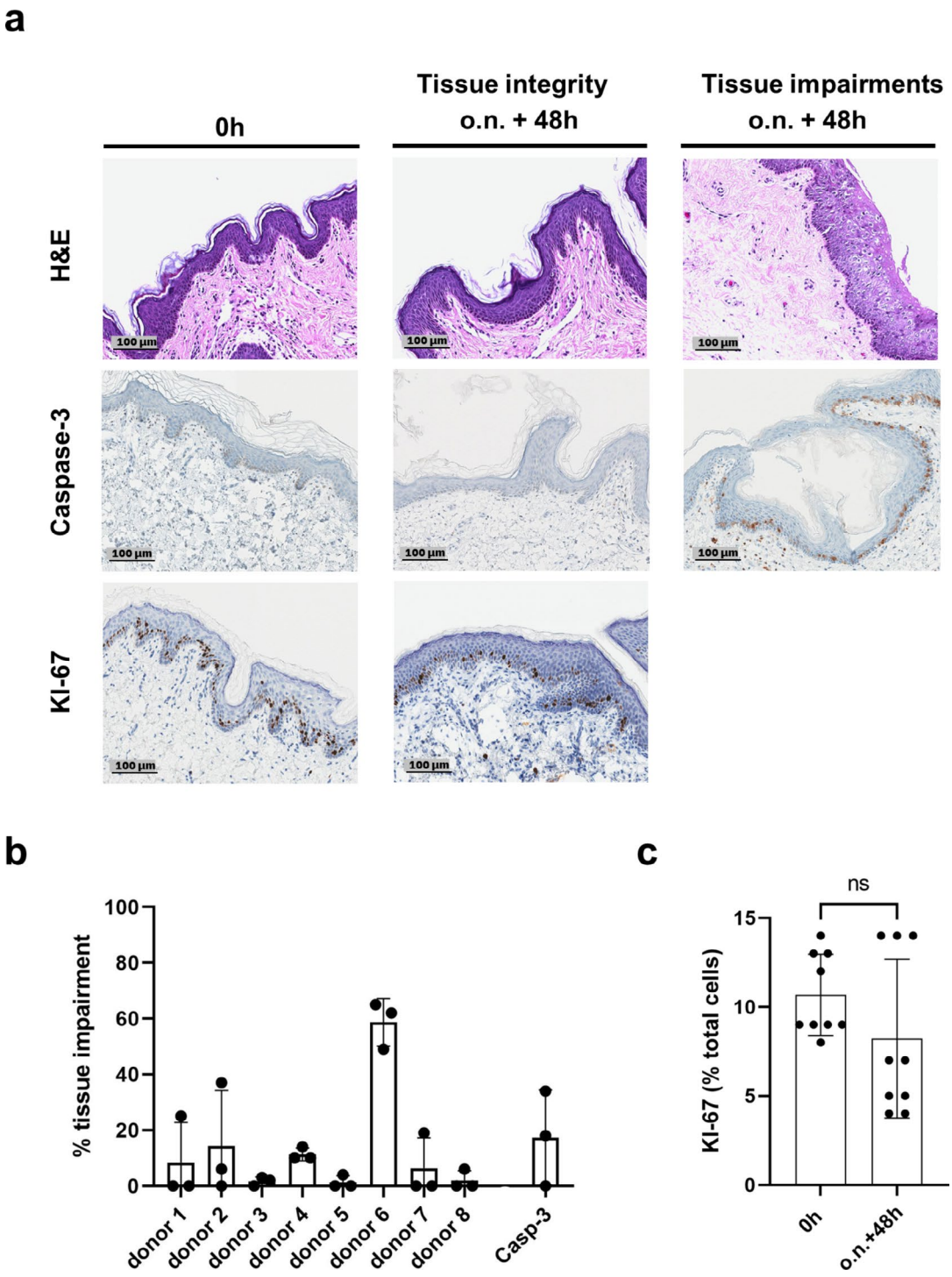

Fig. 3. Preservation of tissue integrity and tissue viability after three days in culture (a) Comparison of haematoxylin and eosin (H&E), Caspase-3 and KI-67 stained skin samples performed at the day of receipt (0 h) and at the end of cultivation (o.n. + 48 h…overnight (19–24 h) + 48 h). For H&E and Caspase-3 exemplary pictures of skin that is well preserved after cultivation time as well examples of damaged skin are presented. Proliferating keratinocytes, marked by a KI-67 staining, are found in the basal layer at both time points. Magnification x20, Scale bar 100 µm. (b) Structural damage and apoptotic cells appear in restricted areas. Impairments are given as a percentage of their lengths over the whole length of the epidermis. H&E: three samples per donor, Caspase-3: three samples of three different donors. (c) Keratinocytes still proliferate at the end of cultivation. Quantitative analysis of KI-67 positive cells in relation to total cell count. $n = 9$. Each time point: three fields of evaluation of one sample per donor, total of three different donors. Mean ± Standard Deviation (SD) of all performed experiments for each time point compared by unpaired two-tailed t-test; ns… not significant.

At the end of cultivation, the punches demonstrated an intact epidermis. Only a focal spongiotic area was seen in some of the punches. Out of the 24 samples analyzed for tissue impairment (Fig. 3b), 10 did not show any disruptions, and further seven had 10 or lower percentage of damaged epidermis. On average 13 % of the epidermis was impaired of the 24 samples analyzed. Within one donor the impairments were incomparable high suggesting issues during cultivation. Viability of epidermal keratinocytes on a histological level was examined by staining for proliferation and apoptosis, using KI-67 and Caspase-3 respectively. Proliferating keratinocytes were found in the basal layer of the epidermis for both time points. Caspase-3 positive staining was restricted to areas similar to tissue structure impairments. With an average of 17 % it lies around the observed percentage of H&E stained tissue damages. Quantitative analysis of KI-67 positive keratinocytes at both time points, beginning and end of cultivation, did not show significant difference.

Immune cells remain constant in the MUG-hOSEC (Medical University of Graz – human Organotypic Skin Explant Culture) model over determined time period

One of the main advantages of utilizing an ex vivo skin model is the presence of cells belonging to the innate and adaptive skin immune system[28]. The preservation of the presence of a set of immune cells; including nucleated hematopoietic cells (B- and T-cells), dendritic cells (Langerhans cells) and macrophages is shown by specific staining (Fig. 4).

The presence of different cell types of the immune system was confirmed by the corresponding staining. Langerhans cells are located in the epidermis, macrophages were located in the dermis. Leucocytes accumulated near the dermal/epidermal interface and in some cases individual cells were seen in the epidermis at both time points. Quantitative analysis of Langerhans cells showed a significant reduction in numbers at the end of the three days cultivation period.

Signals released by the MUG-hOSEC (Medical University of Graz – human Organotypic Skin Explant Culture) model over cultivation time indicate adjustment process followed by stabilization

In addition to histological changes, changes in optical appearance and in secreted factors into the culturing medium were studied (Fig. 5) to monitor cell damage and cell activity during cultivation. IL-8 (Interleukin-8) is released by cells during various signaling processes and does serves as an indicator of cells being active. To illustrate the occurring variance for each of the three secretion factors analyzed, three representative donors were selected to provide a good impression of this variance either in comparison to other donors or within the two skin punches of the same donor. Additionally statistical analysis was performed over different donors.

For the optical evaluation, it can be observed that from the start of cultivation until the next day skin punches noticeably became paler, and from then on, the color remained the same. The factors secreted into the supernatant can be divided into two groups, stabilizing factors (LDH (lactate dehydrogenase) and NTA (Nanoparticle Tracking Analysis) secretion) and activity factors (IL-8 expression). An unspecific secretome analysis by NTA technology provides information on the size distribution and concentration of released total particles into the media of a sample. The highest amount of particles released was always observed during the first incubation period, overnight, after which it declined or remained constant towards the end of cultivation.

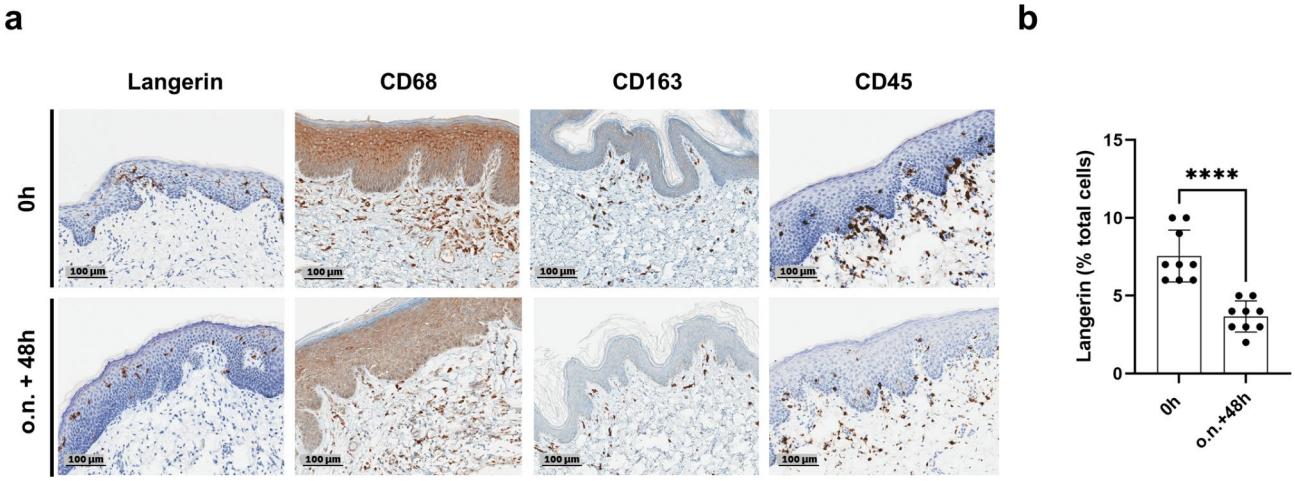

Fig. 4. Immune cells are preserved during three-day cultivation period. (a) Staining's were performed at the day of receipt (0 h) and at the end of cultivation (o.n. + 48 h… overnight (19–24 h) + 48 h). Langerin staining of Langerhans cells; CD68 and CD163 staining of macrophages scattered in the dermis; CD45 staining of leucocytes. Representative image sections were selected. Magnification x20, Scale bar 100 µm. (b) Langerhans cells reduce in number after cultivation period. Quantitative analysis of Langerin positive cells in the epidermis $n = 9$. Each time point: three fields of evaluation of one sample per donor, total of three different donors. Mean ± Standard Deviation (SD) of all performed experiments for each time point compared by unpaired two-tailed t-test; ****… $P < 0.0001$.

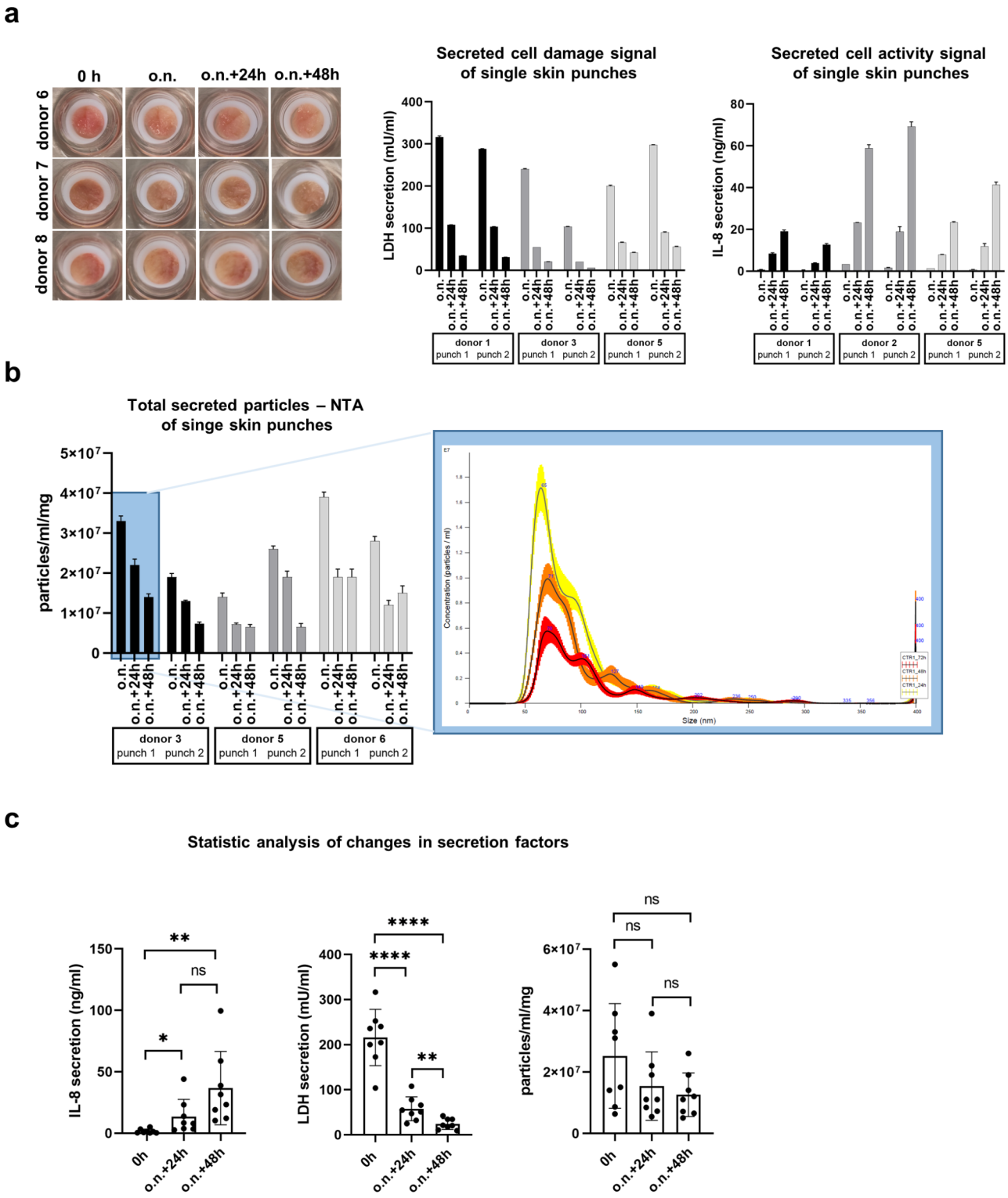

The same trend is evident when examining LDH release into the medium, an enzyme that is released upon cell death. The decrease in all cases results in values below 100 mU/ml at the end of cultivation. In contrast, IL-8 increases over time, reaching varying final levels within one donor and between different donors. All values of all donors are available in the supplementary file Table S1.

Testing of functionality by observing the response to cytotoxic and inflammatory stimuli

The response, and therefore representing the functionality, of the established MUG-hOSEC (Medical University of Graz – human Organotypic Skin Explant Culture) model towards a cytotoxic and inflammatory stimulant was evaluated. Cytotoxic and inflammatory responses were investigated using 1 % SDS (sodium dodecyl sulfate) and LPS (Lipopolysaccharide) in two concentrations (1 and 10 µg/ml). The effects of both agents are visible in Fig. 6.

◂**Fig. 5**. Changes over cultivation time lead to stabilization and show cell activity. Three to four time points: beginning of the experiment (0 h), o.n.… overnight (19–24 h), o.n. + 24 h and o.n. + 48 h (a) Optical changes and changes in cell damage and activity status. Pictures of the same skin punch at four time points. Three donors, one skin punch each per donor. Medium of the MUG-hOSEC model was analyzed at different time points applying LDH (lactate dehydrogenase) release assay and IL-8 (Interleukin-8) ELISA. Three donors, two skin punches each per donor. Mean ± Standard Deviation (SD) of two technical replicates each column. (b) Secretome analysis. Medium of the MUG-hOSEC model was analyzed at different time points by NTA (Nanoparticle Tracking Analysis), unspecific signal of total released particles. Three donors, two skin punches each per donor. Mean ± Standard Deviation (SD) of five technical replicates. NTA results (particles/ml/mg) are normalized to the weight of each skin punch. Exemplary merged NTA result curves of the three time points: yellow = o.n.; orange = o.n. + 24 h; red = o.n. + 48 h (c) Statistical analysis of the secretion factors. $n = 8$; eight different donors; Three time points: o.n.… overnight (19–24 h), o.n. + 24 h and o.n. + 48 h Mean ± Standard Deviation (SD) of all performed experiments for each time point were compared by unpaired two-tailed t-test; ns… not significant, *…$P < 0.05$, **…$P < 0.01$, ***…$P < 0.001$, ****…$P < 0.0001$.

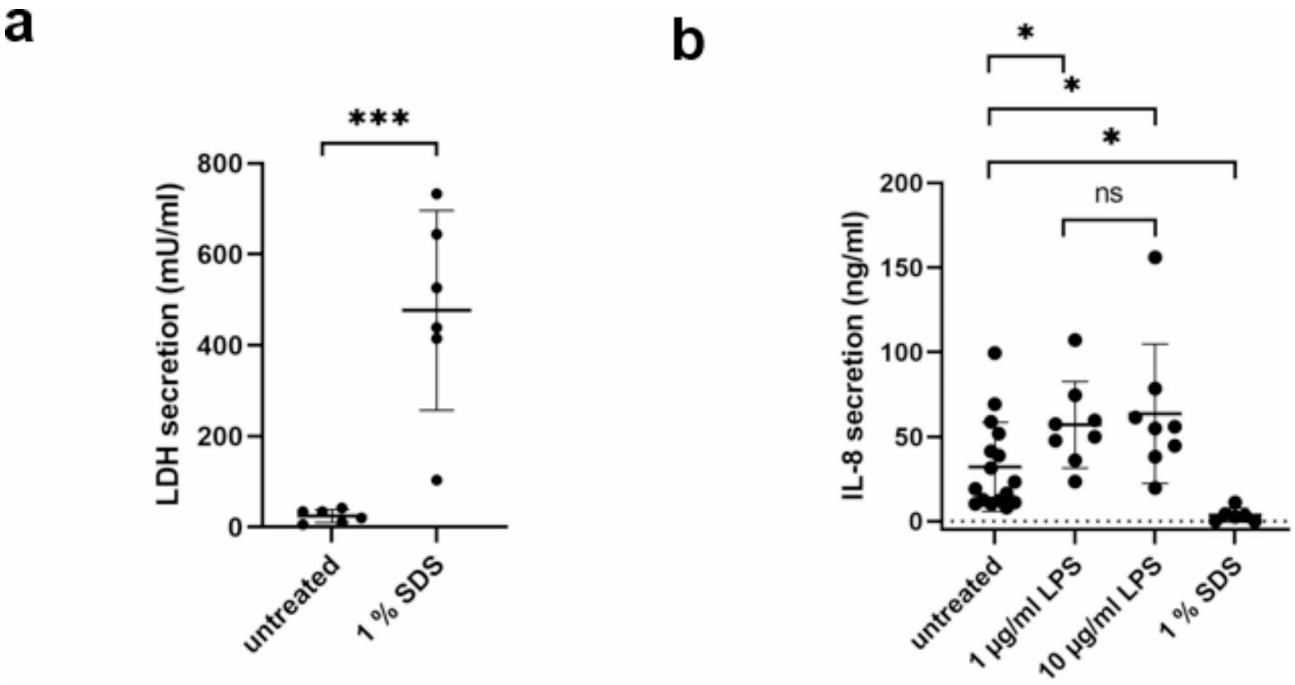

Fig. 6. Response to cytotoxic and inflammatory stimuli measurable in supernatant. (a) LDH (lactate dehydrogenase) secretion elevated by SDS administration. Treatment with 30 µl 1 % SDS for 24 h. $n = 6$; Results of six different donors per condition. Mean ± Standard Deviation (SD) were compared by unpaired two-tailed t-test; ***…$P < 0.001$. Each measurement point is composed of two technical replicates. (b) IL-8 secretion increases upon LPS treatment and decreases with SDS addition. LPS treatment in two concentrations: 1 µg/ml and 10 µg/ml for 48 h and 30 µl 1 % SDS treatment for 24 h. Each point of each condition represents the result of one skin punch of one different donor (the mean value of 2 technical replicates), $n = 16$ for untreated control, $n = 8$ for LPS treated punches and $n = 6$ for SDS treated samples. Mean ± Standard Deviation (SD) of all performed experiments for each condition compared by unpaired two-tailed t-test; ns… not significant, *…$P < 0.05$.

SDS treatment led to significant increase in LDH (lactate dehydrogenase) secretion compared to an untreated control from the same donor (Fig. 6(a)). In contrast, IL-8 (Interleukin-8) secretion, upon SDS treatment, decreased to values below the lowest levels observed in untreated control punches (Fig. 6(b)). The impact of SDS on the skin punches is also visible in the significant increase in concentration and size of nonspecific particles released upon SDS treatment (Nanoparticle Tracking Analysis (NTA) results, see Fig. S1).

The inflammatory response of the MUG-hOSEC model towards LPS is evident in the increase of IL-8 secretion for both concentrations (Fig. 6(b)). The fold increase compared to the control samples is 1.77 for 1 µg/ml and 1.98 for 10 µg/ml. No correlation to NTA results, as for SDS, can be drawn, as the control signal for LPS in medium produced a high background signal (see Fig. S1).

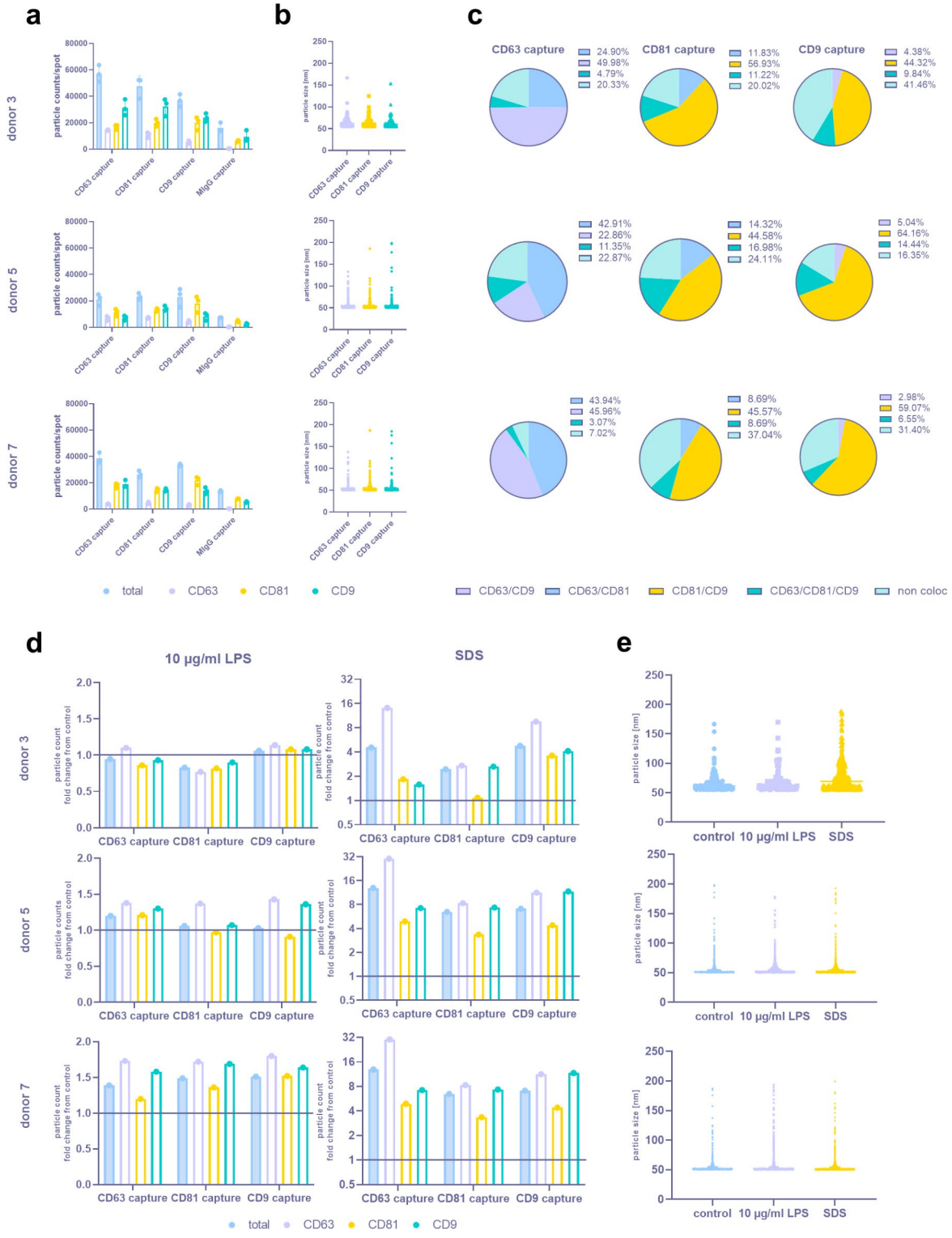

Characterization of MUG-hOSEC (Medical University of Graz – human Organotypic Skin Explant Culture) derived extracellular vesicles by ExoView technology

EVs (extracellular vesicles) are present in human skin and have been reported to contribute to skin homeostasis. They are identified to play a role in cell-cell communication and skin aging[29]. For extensive EV characterization from minimally processed samples we used the ExoView R200 platform based on two overlapping systems: antigenic capture with interferometric imaging and fluorescent antigenic detection on the captured EVs. We immunologically immobilized EVs from the supernatant of the MUG-hOSEC model by the membrane proteins CD9, CD63 and CD81 on a microarray chip. The EVs were counted and sized by light interference down to 50 nm; furthermore immunofluorescence stainings for CD9, CD63 and CD81 were performed to determine the tetraspanin composition at a single vesicle level. Only vesicles with sufficient fluorescence signal were used for analyses. ExoView Analyzer Software was used to set the threshold and discriminate between

◀**Fig. 7**. EVs are released by MUG-hOSEC model. EVs were detected by ExoView technology capturing the three exosome specific tetraspanins: CD9, CD63 and CD81 in three technical replicates. (a) Total fluorescence particle count of donor-derived EVs on tetraspanin capture spots and mouse IgG isotype control analyzed using fluorescence antibodies against CD9, CD63 and CD81. Presented is the Mean ± Standard Deviation (SD) of three technical replicates. (b) Size distribution of donor-derived EVs on tetraspanin capture spots analyzed using the ExoView200 software and are given as single dots for each tetraspanin capture. (c) Tetraspanin colocalization of donors using three fluorescent channels and overlay of fluorescent images, data show the tetraspanin colocalization of all detected EVs. Pie charts indicate the percentage of each tetraspanin colocalization on the released EVs in different colors for the three capturing spots, respectively; non coloc – indicates no colocalization. Concentration is given by particle counts per capture spot of each tetraspanin spot plus internal MIgG control, Mean ± Standard Deviation (SD). (d) Tetraspanin expression in EVs changes upon SDS treatment. EVs derived from skin punches treated with 10 µg/ml LPS or 1 % SDS were compared to EVs release by untreated skin punches of the same donor. Fold change in particle count is given for each of the three tetraspanin capture spots indicating changes in tetraspanin expression. (e) Size distribution of EVs derived from treated skin punches on tetraspanin capture spots analyzed using the ExoView200 software and are given as single dots for each tetraspanin capture.

EVs and contaminations based on the isotype control. The total particle counts per spot are higher in donor 3 (57160 ± 6235 particle counts/CD63 spot, 47547 ± 8090 particle counts/CD81 spot, 36835 ± 4696 particle counts/CD9 spot) compared to donor 5 (21204 ± 4449 particle counts/CD63 spot, 23305 ± 2420 particle counts/CD81 spot, 23124 ± 7089 particle counts/CD9 spot) and donor 7 (38451 ± 4072 particle count/CD63 spot, 26570 ± 2512 particle counts/CD81 spot, 33430 ± 900 particle counts/CD9 spot) (Fig. 7(a)). However, by comparing the initial weight of the samples from the different donors, donor 3 is the heaviest with 115.1 mg followed by donor 5 with 92.6 mg and donor 7 with 77.7 mg (Tab. S1). Although the CD63 spots showed a similar or even higher particle count in all three donors (Fig. 7(a)), more particles tend to be single positive for CD81 compared to CD63 and CD9 ((Fig. 7(c), depicted as non coloc).

The size distribution was very similar for all three donors, most of the particles were captured between 50 and 70 nm. In donor 5 and 7, EVs on the CD9 capture spot appeared more variable in size (Fig. 7(b)).

Focusing on the CD63 spots, as an example for interpretation of the data, donor 3 represents 20.33 % CD63 single positive EVs; 49.98 % are positive for CD63 and CD9, 24.90 % are positive for CD63 and CD81; only 4.79 % were triple positive for all tetraspanins on CD63 spots. 22.87 % of the EVs derived from donor 5 were single captured by the anti-CD63 antibody, 42.91 % were bound to CD63 and the CD81 antibody, 22.86 % from CD63 together with CD9, and 11.35 % were captured from all three antibodies on the CD63 spots. Donor 7 in detail, 43.94 % of CD63 positive EV revealed also a signal for CD81. 45.96 % of CD63 positive EVs were also positive for CD9, and only 3.07 % showed a localization with CD9, CD81 and CD63 on the same vesicle. Only 7.02 % of the CD63 positive EVs were single positive for CD63. Each tetraspanin co-localization pattern of the three donors showed an individual tetraspanin composition, whereby all three tetraspanins could be detected (Fig. 7(c)).

An individual tetraspanin fingerprint, meaning an individual combination of CD63, CD81 and CD9 in various constellations on the released EVs, can be seen when comparing samples of three individual donors. The same pattern of tetraspanin composition is observable upon treatment with LPS in a concentration of 10 µg/ml in all three donors. The fold change in particle counts compared to an untreated control skin punch (Fig. 7(d)) lies around 1 and is portrayed as well in the unaltered co-localization pattern (Fig S2). It further confirms that different skin punches from the same donor do show a similar tetraspanin composition. In contrast, treatment with SDS increased the particle counts in all three donors and all three tetraspanins; especially CD63 shows increased expression (Fig. 7(d)). The particle count fold change from control never exceeds two for LPS treaded skin samples, whereas for SDS treaded skin samples of donor 5 and donor 7 all particle counts are over two-fold in change. For donor 3 this observation is true for nine out of the twelve capture spots. Furthermore, the co-localization pattern (Fig S2) changed upon SDS treatment in each donor, as well. The particle size remains constant around 50 nm for all conditions and donors (Fig. 7(e)).

Discussion

This study provides initial validation data for cultivating an ex vivo skin model under alternative conditions differing from the standard 37 °C in a CO_2 incubator. The research focuses on developing the MUG-hOSEC (Medical University of Graz – human Organotypic Skin Explant Culture) model from foreskin without animal products, CO_2 incubators and at room temperature. This approach enables testing without expensive lab equipment, simplifies handling and makes the model accessible to non-specialists. Additionally, it allows for easier adjustments in environmental influence experiments, which are challenging in a closed system like a CO_2 incubator.

Moreover, we demonstrate a stable release of extracellular vesicles (EVs) from our new designed ex vivo skin model.

Ex vivo skin models imply high heterogeneity, not only between different donors, but as well as within the same donor. In order to better understand the occurring variance within our MUG-hOSEC model we included an overview of structural differences (Fig. 2) as well as differences in the amount of released analytes (Fig. 5). Dependent on the site of excision of the individual skin punch a variation is generated. There are different sets and abundances of resident immune cells in the inner compared to the outer foreskin, as well as differences in keratinization[30–32]. These differences combined with differences in skin appendages present, vascularization

observed, further add up to the heterogeneity. Additionally the endogenous microflora of the skin is part of the individuality of each person and leaves a microbial background even after disinfection of the skin[33]. The general high intra- and inter-variance has to be taken into account when applying an ex vivo skin model and can be compensated by an increase of biological replicates. In Graz, approximately 230 pediatric circumcisions are carried out annually, whereby around 90 % can be used here due to the qualitative conditions, no presence of lichen sclerosus et atrophicus. Within the 90 % not all samples are suitable as they are too small to retrieve skin punches (within this study 11 out of 19 were too small). Although the MUG-hOSEC model faces limitations in sample availability due to the processing requirements and variability observed in certain experimental outcomes, it remains a valuable tool for preliminary studies and hypothesis generation, with sufficient sample capacity for focused research and the potential for scalability through multicenter collaborations. A further improvement in the reliability and reproducibility of the experiments is the most remarkable possible standardization of the media (defined without serum) and of the process, for example short ischemia times, and compliance with standard operation procedures (SOPs) from the operation, to the transport and processing of the samples. As challenging as the variations and difficulties in biological differences in human foreskin samples may be, human experiments are far better compared to the reliability and comparability of animal experiments[34]. There is a significant difference between humans and mice regarding the detailed structure and functions of the individual skin layers. The most visually striking difference is the dense coat of mouse skin with a hair cycle that runs through a defined synchronous cycle, which differs from the asynchronous human hair growth cycle[35]. There are also histological differences: the mouse has a much thinner epidermis and dermis, no sweat glands (except on the paws), and a looser skin bond. Regarding wound healing, mouse skin heals by re-epithelialization due to the more robust contraction component[36].

Despite the heterogeneity challenge, another challenge faced by explant skin cultures is guaranteeing the overall maintenance and conformity during the experimental time frame. The kind and the degree of changes attributed to culturing that can still be tolerated may vary depending on the aim of the studies performed. The balance between degenerative processes and maintaining the organ culture under 37 °C cultivation condition has been shown by different testing strategies. Concluding recommendation for usage duration range from four days[23] up to four weeks[20]. Models used for wound healing need to be reliable for several weeks and pose different requirements compared to models used in toxicity studies, where three days of culturing are sufficient[37].

The maintenance of the MUG-hOSEC model during the experimental time period of three days was evaluated on three levels, optical changes in appearance, histological changes as well as changes of secreted factors relating to the viability and activity status of the skin model. The skin color of the skin punches changed most during this first incubation period. Skin punches got paler, but then on the color did not visibly change. Histological changes of the epidermal keratinocyte layer is a common feature to evaluate degenerative changes of the skin in culture. In the MUG-hOSEC model, the majority of the epidermis was not affected at the end of the cultivation, diagnosed from an experienced pathologist. Impairments in restricted areas were visible as vascularization of keratinocytes and spongiosis. These impairments could derive from a local lack of optimal nutritional supply. In other cases accumulation of spongiosis was found at the edges of the skin punches which may be due to loss of air/liquid cultivation as the skin curved in at those areas.

Spongiosis as a response to cultivation time correlates to observation within the work of other groups[18,19,23], suggesting a common feature of ex vivo skin culturing. It is to be noted that observed alteration in epidermal structure also varies between skin models cultured at 37 °C inside an incubator. In some cases a thickening of the epidermis[19], starting to appear at day four, was noted that was absent in other studies[18]. This suggests an additional strong influence of cultivation technique (for example culturing medium, set-up of air/liquid cultivation), beside other influences such as in our case the altered cultivation temperature. Underlining the observation of a good structural conservation of the MUG-hOSEC model after three days in culture, the epidermis maintained proliferating keratinocytes and exhibited minimal occurrence of apoptotic cells. The general good preservation of the epidermal structure of the MUG-hOSEC model might be attributable to the lower temperatures. There are recent studies suggesting a better conservation of organ culture at low temperatures[38]. The lower temperature may as well lead to a better conservation of resident immune cells. Langerhans cells, the most critical sensors in skin immunity, are known to migrate out of skin explants during the advance of cultivation and thereby be reduced in number. On day three, the amount of Langerhans cells is reduced to about one fourth at cultivation temperatures of 37 °C[39]. Langerhans cells among other immune cells remained within the MUG-hOSEC model on day three (Fig. 4) and were reduced to about half of their original number.

Additionally it must be pointed out that the LDH (lactate dehydrogenase) values, released by damaged cells, decreased over the evaluated three-day cultivation period. Kleszczyński et al. used the LDH release as well to evaluate their skin model at 37 °C during the cultivation time of five days[23]. Both skin models, the one cultivated at 37 °C and the MUG-hOSEC model cultivated at room temperature, showed high initial values after the first day in culture, possibly due to the preparation process, followed by a decrease in both cases. In contrast to the MUG-hOSEC model, where LDH values decreased in the subsequent cultivation days until day three, the model cultivated at 37 °C exhibited an increase in LDH values starting from day three. This might lead again to the conclusion that cells within the skin model at room temperature can be maintained viable for a longer cultivation period.

Before using the MUG-hOSEC model, an equilibration phase overnight (19–24 h) is strongly recommended. Since the NTA (Nanoparticle Tracking Analysis; total particles released) and LDH values show the highest signals during this equilibration phase (Fig. 5) which indicates an adjustment process. As signals in both cases (NTA and LDH) decline until day three, showing the lowest value on day three, it is recommendable to use day three as endpoint for evaluating effects of added substances. For example, the difference between untreated skin and skin treated with a cytotoxic agent is increased due to the lower background signal, increasing sensitivity of the model.

In contrast to NTA and LDH values, IL-8 (Interleukin-8) values increase over the evaluated cultivation time of three days. In ex vivo skin models specific released cytokines can be regarded as a viability and activity indicator of cells sending out signals for wound healing and proliferation after surgery, concluded by a metabolic study performed by Neil et al.[18]. This increase of cytokine release over time, can also be observed within reconstructed skin equivalent models[40,41], attributable to proliferating underlying the contribution of cytokines in various pathways. Interestingly, when comparing IL-8 values of skin samples from different body sites (foreskin and abdominal skin) cultured at 37 °C at the same time point (48 h) a huge difference in absolute values can be observed. Foreskin samples exhibit values roughly between 50 and 250 ng/ml[42] and abdominal samples roughly between 0 and 50 ng/ml[22]. This suggest a higher activity of foreskin cells compared to abdominal skin cells. The IL-8 values of the MUG-hOSEC model at room temperature are roughly between 0 and 45 ng/ml around 48 h of cultivation, suggesting a lower activity of foreskin cells at room temperature compared to foreskin cells at 37 °C. Within the study of Danso et al. a similar effect of temperature on their ex vivo wound healing skin model was observed[43]. Proliferation, necessary for skin repair, was delayed for skin cultivated at 32 °C compared to skin cultivated at 37 °C. Signaling processes seem to be attenuated by lowering the temperature. We consider our MUG-hOSEC model less as a wound healing or barrier repair model, but rather as a model that is valued for its stability and flexibility in toxicity and inflammation studies.

In addition to maintaining a good conservation over the cultivation time the MUG-hOSEC model did react towards external stimuli. 1 % SDS (sodium dodecyl sulfate, cytotoxic agent) application resulted in a significant increase in LDH. As the SDS was not contained on the epidermis but tripped into the culturing media the signal obtained is derived from its adverse effect on the whole skin punch including epidermal and dermal cells. In order to trace back the signal exclusively towards topical exposure, adjustments in the model need to be made. We introduced a Teflon ring into our commercially available trans-well inserts to create a better contrast for optical evaluations. For further testing on the topical effect of substances a funnel construction could help sealing off the epidermis and retain substances from tripping into the media. Such a simple construction was performed by Roger et al. using a commercially available cloning rings[44].

The potential to induce inflammation in the MUG-hOSEC model was investigated using LPS (Lipopolysaccharide) in two concentrations 1 and 10 µg/ml. In both cases IL-8 secretion levels increased significantly. A dose dependency by these two concentrations as in the study of Gvirtz et al. was not observed, neither was the fold increase as high as for their assessment using 5 µg/ml LPS for 48 h[22]. The significant increase in the MUG-hOSEC model was observable in samples treated for a duration of 48 h. After the first 24 h of treatment, no effect was observable, again giving a hint towards delayed responses in the system.

Extracellular vesicle (EV) research is relatively new but growing and is undoubtedly a part of cell communication that is essential in obtaining a complete picture of cell signaling[45] and therefore should not be neglected in ex vivo skin culturing. Especially since EVs are of great importance for clinical and translational applications[46,47]. To detect EVs in our MUG-hOSEC model, we chose next-generation EV analysis device, the single-particle interferometric reflectance imaging ExoView R200 platform which exclusively captures and analyses EVs via their characteristic membrane proteins, tetraspanin CD9, CD63 and CD81[48]. Nakamura et al. examined the role of EVs released by the skin disease systemic sclerosis[49]. In vitro experiments with healthy and diseased fibroblasts did show an alteration in the tetraspanin markers of released EVs. The protein levels of CD9, CD63 and CD81 were increased in affected fibroblasts. Additionally, CD63 mRNA levels were significantly upregulated and total EVs release increased. These described changes for systemic sclerosis derived fibroblasts were also observed within our study upon SDS treatment of juvenile skin punches.

We would like to point out that the EV secretion is measured from all cells represented in the skin model and differ compared to only one cell type, e.g. a fibroblast cell line. In total, there was an increase in numbers of EVs released upon SDS treatment. This change in tetraspanin composition and quantity might derive from cells adjacent to the dying cells, as cell death can lead to inflammatory reactions[50,51], sending out recruiting signals. In contrast, LPS treatment did not result in changes within tetraspanin expression, suggesting an alternative mechanism. Possible explanations might be that not the tetraspanin composition is effected, but that the cargo carried by the EVs differs, or the time point of harvest is not ideal. SDS might impose a severer threat resulting in a stronger signal. However, the fraction of EVs released by immune cells upon LPS treatment, in relation to the total amount of cells present and releasing EVs, could be too small to be noticed by tetraspanin analysis.

In conclusion, the MUG-hOSEC ex vivo skin model, derived from juvenile foreskin can be maintained at room temperature and remains reactive to external stimuli. The model releases extracellular vesicles (EVs) into the supernatant, providing valuable information on skin cell status. Standardizing the process, and increasing the number of tests and quality controls are necessary to address endogenous heterogeneity. While the lower cultivation temperature can delay degradative processes, it may also limit the model's applications. These preliminary findings support further specific validations for potential applications.

Methods

Experimental design

Of all the foreskin samples received, in total 19, eight foreskins were selected appropriate to conduct the experiments, in 11 cases no punches could be retrieved from the skin, as they were too small. After an overnight (19–24 h) equilibration phase with medium only, individual skin punches were treated with LPS (Lipopolysaccharide from *E.Coli* O55:B5; MedChemExpress) in two concentrations: 1 and 10 µg/ml. This treatment was repeated after the first 24 h, resulting a total treatment duration of 48 h. Concentrations and treatment duration were derived from previous work performed on the kinetics of LPS towards an ex vivo skin model[22]. In contrast, 1 % SDS (sodium dodecyl sulfate in PBS; Sigma Aldrich) was added only once during the last 24 h of the cultivation period. 30 µl of the 1 % SDS solution were pipetted onto the epidermis of the

skin punches. With time, the solution tripped into the culturing medium provided in the 6-well plate. Each experiment included two untreated samples to represent inter-assay variability.

Juvenile human skin explant culture

Skin samples used within this study were obtained from circumcisions of boys (age range: 0–17 years) performed at the Pediatric and Adolescent Surgical Department of the hospital in Graz. following signature of an informed consent by the patients and/or parents. Samples were only taken from skin without pathologic morphological changes. The ethic committee of the Medical University of Graz granted associated approval (31–528 ex 18/19 1358–2019). All experiments were performed in accordance with the relevant guidelines and regulations.

The operations were performed according to common procedures, Betaisodona disinfection solution was used prior to operation. After operation, the anonymized skin samples were stored in DMEM (Gibco, Life Technologies, Darmstadt, Germany) medium without supplements and cooled at 4 °C until further processing within at least 24 h. Washing and disinfections steps under sterile conditions (3x washing with PBS before incubation in 10 % Penicillin/Streptomycin for 10 min at room temperature, additional 1x washing with PBS) preceded cutting the skin tissue into circles using an 8 mm skin punch. In order to allow an air-liquid cultivation, the skin punches were placed into trans-well inserts (Millicell Cell Culture Insert, 12 mm, polycarbonate, 0.4 µm; PIHP01250) with the epidermis facing up. The trans-well inserts were modified by the insertion of a teflon ring, manufactured in house by the Prototyping and Construction Department of the Medical University of Graz. These rings fit close to the wall of the inserts (outer diameter: 9 mm / inner diameter: 7 mm / slope outside towards inside: 45°). The white ring provides contrast for better optical evaluation of the skin in culture. The skin punches were placed into these rings. For cultivation the inserts were placed in one well of a 6-well plate filled with 1.5 ml of cultivation medium. Cultivation medium was CO_2 independent base media supplemented with 1 % L-Glutamine, 1 % non-essential amino acids, 1 % ITS (Insulin-Transferrin-Selenium) and 10 ng/ml hydrocortisone, based on a serum-free media used in the incubator[24]. No antibiotics were added. The base media, CO_2 independent media, was purchased from Gibco (catalog no.: 18045088), this media does not contain a HEPES buffering system, instead it contains a unique buffering system composed of mono and dibasic sodium phosphate and β-glycerophosphate capable of maintaining long term pH stability under atmospheric CO_2. All above stated supplements to the base media were purchased from Gibco (Gibco, Life Technologies, Darmstadt, Germany), except hydrocortisone from Stemcell (Stemcell Technologies™, Cambridge). For a short workflow overview refer to Fig. 1. Medium was changed daily. The model was placed inside the lab at room temperature (21–23 °C). At the conclusion of each experiment, a sterility test of the skin punch in culture was conducted. The skin punches were taken out of the inserts and transferred in a 6-well plate filled with 3 ml of cultivation medium. After gently swirling the punches with sterile forceps a few times, they were retrieved for further histological analysis. The medium for sterility testing was allowed to stand at room temperature for a minimum of 48 h. Within this study none of the antibiotic-free medium surrounding the trans-well insert was contaminated, but after sterility control 5 out of 39 skin punches resulted in bacteria growth. A possible explanation is that the trans-well insert with a pore size of 0.4 µm could serve as a sterile filter, retaining bacteria on the explant. The data generated by these five skin punches was included within the study to provide the most transparency of the model performances.

Analysis of supernatant

For IL-8 (Interleukin-8) and LDH (Lactate Dehydrogenase) quantification, 200 µL aliquots of the supernatant were stored at -80 °C, and one aliquot was used per analysis. The aliquots were either frozen undiluted (IL-8) or in a 1:25 dilution in LDH storage buffer for LDH analysis. Both assays were performed according to the manufacturer's recommendations (Human IL-8 ELISA Set 555244; BD Biosciences and LDH-Glo™ Cytotoxicity Assay; Promega J2380).

Histological analysis

After conducting the experiments, all skin punches were fixated in 4 % formalin for at least 24 h and paraffin embedded according to standard procedures using TissueTek® VIP™ (Sakura®). The skin punches were cut through the middle of the circle and orientated with the cutting size down for pouring into paraffin blocks. 4 µm slides were H&E (haematoxylin and eosin) stained according to standardized protocols. In short, after deparaffinization and rehydration, slides were incubated for 8 min in haematoxylin followed by 10 min incubation under rinsing tap water, then slides were tipped into eosin 10 times following a dehydration series, clearing and finally mounting. Immunohistochemistry was kindly performed by the D&R Institute of Pathology, Medical University of Graz. Refer to Table 1 for staining details.

Tissue integrity was assessed by examining changes in the epidermis through H&E staining. The untreated skin punches, after three days in culture, were examined for the appearance of tissue impairments compared to the skin from the same donor at the beginning of cultivation. Using the software ImageScope x64 (scanned by Aperio Slide Scanner, Leica) the total length of the epidermis was measured by applying the ruler tool through the middle of the epidermis. For each identified tissue impairment, the corresponding length of this section was then related to the total length of the epidermis. The same way of evaluation was performed for Caspase-3 stainings. Changes in the IHC staining profile was assessed by presence and absence of staining in the skin punches obtained at the beginning of the experiment compared to the staining at the end. The IHC staining of KI-67 and Langerin were quantified using QuPath! Software (v0.4.4). Three field distributed over the whole length of the epidermis were analyzed giving percentage positive stained cells of all cells present.

Antibody	Species	Dilution	Sec AK	AK incubation	Pre-treatment	Detection System	Platform	Distributor
Casp-3	Polyclonal rabbit	1:1000		32 min	Ventana CC1 mild	Ventana ultraViewDAB	Ventana Benchmark Ultra	Cell Signaling
KI-67	Monoclonal mouse (MIB1)	ready to use		20 min	low ph 97 °C	DAKO OMNIS Flex (DAB)	DAKO OMNIS	Agilent
Langerin	Monoclonal mouse (12D6)	1 + 100	mouse linker	20 min	low ph 95 °C	DAKO OMNIS Flex (DAB)	DAKO OMNIS	Novocastra
CD45	Monoclonal mouse (2B11 + PD7/26)	ready to use	mouse linker	20 min	high ph 97 °C	DAKO OMNIS Flex (DAB)	DAKO OMNIS	Agilent
CD68	monoclonal mouse (KP-1)	ready to use		20 min	Ventana CC1 standard	Ventana ultraViewDAB	Ventana Benchmark Ultra	Ventana
CD163	Monoclonal mouse (MRQ-26)	ready to use		32 min	Ventana CC1 standard	Ventana ultraViewDAB	Ventana Benchmark Ultra	Ventana

Table 1. Summary of IHC staining.

Detection of extracellular vesicles

Unpurified supernatants (200 µl aliquots, stored at -80 °C) from the ex vivo models were taken and measured using NTA (Nanoparticle Tracking Analysis) technology to obtain an approximate estimate of the concentration of whole particles present for subsequent ExoView analysis. A separate aliquot was taken for each analysis.

Nanoparticle tracking analysis (NTA)

The NS300 Nanosight (Malvern Panalytical, Malvern) was used with a 405 nm laser filter. Samples were diluted 1:5 with PBS prior application. Five 60 s videos were used to create a merged curve by the NTA software 3.2. When the result of one video was deemed unreliable by the software, four videos were used for the creation of the merged result (7 out of 70 results affected).

ExoView analysis

EVs (extracellular vesicles) are captured and measured by the ExoView technology. ExoView R200 (NanoView Biosciences) was used to analyze collected medium from the ex vivo skin models stored at -80 °C. Microarray chips coated with anti-tetraspanin antibodies against CD9, CD63, CD81 and mouse IgG as isotype control (Leprechaun Exosome Human Tetraspanin Kit 251–1044; LOT 032472001E and 032472001 F, Unchained Labs) were pre-scanned according to the manufacturer´s instruction to generate a baseline before sample incubation. To sediment cellular debris, the supernatants were centrifuged at 2,500xg for 5 min. Supernatants of control, 10 µg/ml LPS treatment and SDS treatment from three donors (donor 3, donor 5, donor 7) each were diluted 1:50 in Incubation Solution provided in the kit. 50 µl in total were loaded onto the pre-scanned chips and incubated over night at room temperature. After incubation, antibody staining was performed according to the user guideline provided by the manufacturer. In brief, all incubation steps were performed with gentle shaking. First, microarray chips were washed three-times with solution A (Kit 251–1044); secondly, antibody mixture with all three anti-tetraspanin antibodies was prepared and incubated for one hour at room temperature protected from light. Unbound antibodies were washed by washing once with solution A, three times with solution B (Kit 251–1044) and a final washing step with aqua dest. After drying the chips, they were finally transferred to the sample stage for fluorescence and interferometric imaging. Data were analyzed using the ExoView Analyzer Software (NanoView Biosciences).

Statistical analysis

All data are reported as Mean ± SD (Standard Deviation). The number of independent experiments (n) and technical replicates is indicated below the graphs. Statistical analysis were performed using an unpaired, two-tailed t-test (GraphPad Prism 9.0.0) P-value: significant *($P < 0.05$); highly significant **($P < 0.01$); extremely significant ***($P < 0.001$) and ****($P < 0.0001$).

Due to the high inter- and intra-variability of the experiments no direct comparison of untreated to treated readouts of the results of individual skin punches within one experiment was performed. Instead, a pooled comparison of the mean values of all results of all performed experiments of one condition is considered more appropriate to elucidate a result that represents a significant tendency.

Data availability

The data that support the findings of this study are available from the corresponding author upon reasonable request.

Received: 1 August 2024; Accepted: 3 October 2024
Published online: 14 October 2024

References

1. OECD. 431: in Vitro skin corrosion: human skin model test. *OECD Publishing Paris*. https://doi.org/10.1787/9789264071148-en (2004).
2. OECD. 439: in Vitro skin irritation: Reconstructed Human Epidermis Test Method. *OECD Publishing Paris*. https://doi.org/10.1787/9789264090958-en (2010).

3. Hofmann, E., Schwarz, A., Fink, J., Kamolz, L. P. & Kotzbeck, P. Modelling the complexity of human skin in vitro. *Biomedicines*. **11**, 794. https://doi.org/10.3390/biomedicines11030794 (2023).
4. Varani, J. Human skin organ culture for assessment of chemically induced skin damage. *Expert Rev. Dermatol.* **7**, 295–230 (2012).
5. Jacobs, J. J., Lehé, C. L., Hasegawa, H., Elliott, G. R. & Das, P. K. Skin irritants and contact sensitizers induce Langerhans cell migration and maturation at irritant concentration. *Exp. Dermatol.* **15** (6), 432–440 (2006).
6. Bergers, L. I. J. C. et al. Immune-competent human skin disease models. *Drug Discov. Today* **21**(9), 1479–1488 (2016).
7. Sarama, R. et al. In vitro disease models for understanding psoriasis and atopic dermatitis. *Front. Bioeng. Biotechnol.* **10**, 80321. https://doi.org/10.3389/fbioe.2022.803218 (2022).
8. Pérez-Salas, J. L. et al. In vitro and ex vivo models for screening topical anti-inflammatory drugs. *Sci. Pharm.* **91** (20). https://doi.org/10.3390/scipharm91020020 (2030).
9. Liu, X. et al. Utilization of *ex vivo* tissue model to study skin regeneration following microneedle stimuli. *Sci. Rep.* **12**, 18115. https://doi.org/10.1038/s41598-022-22481-w (2022).
10. Seiser, S. et al. Comparative assessment of commercially available wound gels in ex vivo human skin reveals major differences in immune response-modulatory effects. *Sci. Rep.* **12**, 17481. https://doi.org/10.1038/s41598-022-20997-9 (2022).
11. Smith, S. H. et al. Development of a topical treatment for psoriasis targeting RORγ: from bench to skin. *PloS One*. **11** (2), e014799. https://doi.org/10.1371/journal.pone.0147979 (2016).
12. Corzo-León, D. E., MacCallum, D. M. & Munro, C. A. Host responses in an ex vivo human skin model challenged with Malassezia sympodialis. *Front. Cell. Infect. Microbiol.* **10**, 561382. https://doi.org/10.3389/fcimb.2020.561382 (2021).
13. Esterly, A. T., Lloyd, M. G., Upadhyaya, P., Moffat, J. F. & Thangamani, S. A human skin model for assessing arboviral infections. *JID Innov.: Skin. Sci. Mol. Popul. Health* **2**(4), 100128. https://doi.org/10.1016/j.xjidi.2022.100128 (2022).
14. Pearton, M. et al. Changes in human langerhans cells following intradermal injection of influenza virus-like particle vaccines. *PloS One*. **5** (8), e12410. https://doi.org/10.1371/journal.pone.0012410 (2010).
15. Roberts, W. Air pollution and skin disorders. *Int. J. Women's Dermatol.* **7**(1), 91–97 (2020).
16. Patatian, A. et al. Skin biological responses to urban pollution in an ex vivo model. *Toxicol. Lett.* **348**, 85–96 (2021).
17. Burke, K. E. Protection from environmental skin damage with topical antioxidants. *Clin. Pharmacol. Ther.* **105** (1), 36–38 (2019).
18. Neil, J. E., Brown, M. B. & Williams, A. C. Human skin explant model for the investigation of topical therapeutics. *Sci. Rep.* **10**, 21192. https://doi.org/10.1038/s41598-020-78292-4 (2020).
19. Xu, W. et al. Application of a partial-thickness human ex vivo skin culture model in cutaneous wound healing study. *Lab. Invest.* **92** (4), 584–599 (2012).
20. Steinstraesser, L. et al. A human full-skin culture system for interventional studies. *Eplasty*. **9**, e5 (2009).
21. Jardet, C. et al. Development and characterization of a human Th17-driven ex vivo skin inflammation model. *Exp. Dermatol.* **29** (10), 993–1003 (2020).
22. Gvirtz, R., Ogen-Shtern, N. & Cohen, G. Kinetic cytokine secretion profile of LPS-induced inflammation in the human skin organ culture. *Pharmaceutics*. **12** (4), 299. https://doi.org/10.3390/pharmaceutics12040299 (2020).
23. Kleszczyński, K. & Fischer, T. W. Development of a short-term human full-thickness skin organ culture model in vitro under serum-free conditions. *Arch. Dermatol. Res.* **304** (7), 579–587 (2012).
24. Sidgwick, G. P., McGeorge, D. & Bayat, A. Functional testing of topical skin formulations using an optimised ex vivo skin organ culture model. *Arch. Dermatol. Res.* **308** (5), 297–308 (2016).
25. Terlecki-Zaniewicz, L. et al. Extracellular vesicles in human skin: cross-talk from senescent fibroblasts to keratinocytes by miRNAs. *J. Invest. Dermatol.* **139** (12), 2425–2436e5 (2019).
26. Wang, M. et al. Skin cell-derived extracellular vesicles: a promising therapeutic strategy for cutaneous injury. *Burns Trauma*. **10**, tkac037. https://doi.org/10.1093/burnst/tkac037 (2022).
27. Nasiri, G., Azarpira, N., Alizadeh, A., Goshtasbi, S. & Tayebi, L. Shedding light on the role of keratinocyte-derived extracellular vesicles on skin-homing cells. *Stem Cell Res. Ther.* **11** (1), 421. https://doi.org/10.1186/s13287-020-01929-8 (2020).
28. Yazdi, A. S., Röcken, M. & Ghoreschi, K. Cutaneous immunology: basics and new concepts. *Semin. Immunopathol.* **38** (1), 3–10 (2016).
29. Wu, H. et al. Extracellular vesicle: A magic lamp to treat skin aging, refractory wound, and pigmented dermatosis?. *Front. Bioeng. Biotechnol.* **10**, 1043320. https://doi.org/10.3389/fbioe.2022.1043320 (2022).
30. Lemos, M. P. et al. The inner foreskin of healthy males at risk of HIV infection harbors epithelial CD4+CCR5+cells and has features of an inflamed epidermal barrier. *PloS One*. **9** (9), e108954. https://doi.org/10.1371/journal.pone.0108954 (2014).
31. Liu, A. et al. Differential compartmentalization of HIV-targeting immune cells in inner and outer foreskin tissue. *PloS One*. **9** (1), e85176. https://doi.org/10.1371/journal.pone.0085176 (2014).
32. Qin, Q. et al. Langerhans' cell density and degree of keratinization in foreskins of Chinese preschool boys and adults. *Int. Urol. Nephrol.* **41** (4), 747–753 (2009).
33. Larson, P. J., Chong, D., Fleming, E. & Oh, J. Challenges in developing a human model system for skin Microbiome Research. *J. Invest. Dermatol.* **141** (1), 228–231e4 (2021).
34. Salgado, G., Ng, Y. Z., Koh, L. F., Goh, C. S. M. & Common, J. E. Human reconstructed skin xenografts on mice to model skin physiology. *Differ. Res. Biol. Divers.* **98**, 14–24 (2017).
35. Paus, R. A comprehensive guide for the recognition and classification of distinct stages of hair follicle morphogenesis. *J. Invest. Dermatol.* **113** (4), 523–532 (1999).
36. Wong, V. W., Sorkin, M., Glotzbach, J. P., Longaker, M. T. & Gurtner, G. C. Surgical approaches to create murine models of human wound healing. *J. Biomed. Biotechnol.* **2011**, 969618. https://doi.org/10.1155/2011/969618 (2011).
37. Vostálová, J. et al. Comparison of various methods to analyse toxic effects in human skin explants: rediscovery of TTC assay. *J. Photochem. Photobiol. B.* **178**, 530–536 (2018).
38. Yuta, T. et al. Development of a novel ex vivo organ culture system to improve preservation methods of regenerative tissues. *Sci. Rep.* **13** (1), 3354. https://doi.org/10.1038/s41598-023-29629-2 (2023).
39. Ng, K. W. et al. Development of an ex vivo human skin model for intradermal vaccination: tissue viability and Langerhans cell behaviour. *Vaccine*. **27** (43), 5948–5955 (2009).
40. Szymański, Ł. et al. A simple method for the production of human skin equivalent in 3D, Multi-cell Culture. *Int. J. Mol. Sci.* **21** (13), 4644. https://doi.org/10.3390/ijms21134644 (2020).
41. Arlian, L. G. & Morgan, M. S. Immunomodulation of skin cytokine secretion by house dust mite extracts. *Int. Arch. Allergy Immunol.* **156** (2), 171–178 (2011).
42. Hippchen, Y. et al. Cultured human foreskin as a Model System for evaluating Ionizing Radiation-Induced skin Injury. *Int. J. Mol. Sci.* **23** (17), 9830. https://doi.org/10.3390/ijms23179830 (2022).
43. Danso, M. O., Berkers, T., Mieremet, A., Hausil, F. & Bouwstra, J. A. An ex vivo human skin model for studying skin barrier repair. *Exp. Dermatol.* **24** (1), 48–54 (2015).
44. Roger, M. et al. Bioengineering the microanatomy of human skin. *J. Anat.* **234** (4), 438–455 (2019).
45. Kalluri, R. & LeBleu, V. S. The biology, function, and biomedical applications of exosomes. *Science (New York, N.Y.)*. 367(6478), eaau6977. (2020). https://doi.org/10.1126/science.aau6977
46. Properzi, F., Logozzi, M. & Fais, S. Exosomes: the future of biomarkers in medicine. *Biomark. Med.* **7** (5), 769–778 (2013).
47. Wiklander, O. P. B., Brennan, M. Á., Lötvall, J. & Breakefield, X. O. Andaloussi, S. advances in therapeutic applications of extracellular vesicles. *Sci. Transl. Med.* **11** (492), eaav8521. https://doi.org/10.1126/scitranslmed.aav8521 (2019).

48. Breitwieser, K. et al. Detailed characterization of small extracellular vesicles from different cell types based on tetraspanin composition by ExoView R100 platform. *Int. J. Mol. Sci.* **23** (15), 8544. https://doi.org/10.3390/ijms23158544 (2022).
49. Nakamura, K. et al. Altered expression of CD63 and exosomes in scleroderma dermal fibroblasts. *J. Dermatol. Sci.* **84** (1), 30–39 (2016).
50. Kono, H. & Rock, K. L. How dying cells alert the immune system to danger. *Nat. Rev. Immunol.* **8** (4), 279–289 (2008).
51. Yang, Y., Jiang, G., Zhang, P. & Fan, J. Programmed cell death and its role in inflammation. *Mil. Med. Res.* **2**, 12. https://doi.org/10.1186/s40779-015-0039-0 (2015).

Author contributions

Author contributionsA.W. designed the study; performed the skin model and wrote the manuscript. C.K. performed the EV data, D.V. prepared the figures and statistics; M.P designed the culture ring; G.S. provided the fore skin samples; B.A. performed the immunohistochemistry, B.R. was responsible for developing the concept, study design, research ethics and funding. All authors reviewed the manuscript.

Declarations

Competing interests

The authors declare no competing interests.

Additional information

Supplementary Information The online version contains supplementary material available at https://doi.org/10.1038/s41598-024-75291-7.

Correspondence and requests for materials should be addressed to B.R.

Reprints and permissions information is available at www.nature.com/reprints.

Publisher's note Springer Nature remains neutral with regard to jurisdictional claims in published maps and institutional affiliations.